Effects of Cytochalasin, Phalloidin, and pH on the Elongation of Actin Filaments†

Prakash Sampath and Thomas D. Pollard*

Department of Cell Biology and Anatomy, Johns Hopkins Medical School, 725 North Wolfe Street, Baltimore, Maryland 21205

Received September 6, 1990; Revised Manuscript Received November 1, 1990

ABSTRACT: We used electron microscopy to measure the effects of cytochalasins, phalloidin, and pH on the rates of elongation at the barbed and pointed ends of actin filaments. In the case of the cytochalasins, we compared the effects on ATP- and ADP–actin monomers. Micromolar concentrations of either cytochalasin B (CB) or cytochalasin D (CD) inhibit elongation at both ends of the filament, about 95% at the barbed end and 50% at the poninted end, so that the two ends contribute about equally to the rate of growth. Half-maximal inhibition of elongation at the barbed end is at 0.1 μM CB and 0.02 μM CD for ATP–actin and at 0.1 μM CD for ADP–actin. At the pointed end, CD inhibits elongation by ATP–actin and ADP–actin about equally. At high (2 μM) concentrations, the cytochalasins reduce the association and dissociation rate constants in parallel for both ADP- and ATP–actin, so their effects on the critical concentrations are minimal. These observations confirm and extend those of Bonder and Mooseker [Bonder, E. M., & Mooseker, M. S. (1986) *J. Cell Biol. 102*, 282–288]. The dependence of the elongation rate on the concentration of both cytochalasin and actin can be explained quantitatively by a mechanism that includes the effects of cytochalasin binding to actin monomers [Godette, D. W., & Frieden, C. (1986) *J. Biol. Chem. 261*, 5974–5980] and a partial cap of the barbed end of the filament by the complex of ADP–actin and cytochalasin. Phalloidin reduces the dissociation rate constants at both ends to near zero and also reduces the association rate constant at the barbed end by about 50%. This confirms and extends the observations of Coluccio and Tilney [Coluccio, L. M., & Tilney, L. G. (1984) *J. Cell Biol. 99*, 529–535] and provides convincing evidence that phalloidin affects both subunit binding and dissociation. Over the pH range of 6.6–8.3, the pH has very little effect on the association rate constant at the barbed end, but the dissociation rate constant is larger at alkaline pH. At the pointed end, the association rate constant decreases slightly at alkaline pH. Together, these effects account for the higher critical concentration and slower rates of polymerization at alkaline pHs.

Two classes of drugs, the cytochalasins and the phallotoxins, have been valuable in evaluating both the mechanism of actin polymerization and the functions of actin in live cells [reviewed by Cooper (1987)]. Although much has been learned, there remain a number of questions regarding the mechanisms of action of these drugs; until they are resolved, the interpretation of many previous studies will be uncertain.

For several years, it has been widely accepted that cytochalasins bind with high affinity ($K_d < 0.1$ μM) to the barbed end of actin filaments, thereby inhibiting strongly or completely both monomer addition and loss (Brenner & Korn, 1979; Brown & Spudich, 1979; Flanagan & Lin, 1980; MacLean-Fletcher & Pollard, 1980; Lin et al., 1980; Pollard & Mooseker, 1981).

This simple mechanism has received two different challenges. First, Mooseker and Bonder (1986) used electron microscopy to demonstrate that 2 μM cytochalasin B (CB)[1] or cytochalasin D (CD) slows, but does not completely stop, elongation at the barbed end of actin filaments. Second, Goddette and Frieden (1986a,b) showed that high concentrations of CD bind to and alter the properties of actin monomers. The dissociation constant is 2–20 μM depending on the divalent cations bound to the actin monomer. CD binding causes a conformational change in Mg-ATP–actin monomers and the formation of dimers that promote nucleation and hydrolyze ATP more rapidly than actin monomers without CD. Third, Carlier et al. (1986) reported that in an elongation assay with ATP–actin monomers, the apparent inhibition constant for CD varied with the concentration of ATP–actin. They proposed two different explanations. First, the nucleotide composition of subunits near the end of the polymer could influence the affinity of CD for the end of the filament, with the affinity being low for ATP–actin and high for ADP–actin. If nucleotide hydrolysis occurs at a constant rate, then polymers growing slowly at low actin concentrations would have a higher proportion of ADP subunits near their ends than rapidly growing filaments. Alternatively, CD might bind to actin dimers so that at high actin concentrations more dimers would be present to bind cytochalasin and less cytochalasin would be available to cap the ends of filaments.

These challenges to the simple barbed end capping mechanism prompted us to reexamine the elongation of actin filaments in the presence of cytochalasins. We have confirmed the observations of Bonder and Mooseker with ATP–actin and added new observations on ADP–actin. Cytochalasin inhibition of actin filament elongation cannot be explained by barbed end capping alone. The capping is incomplete, and other factors inhibit reactions at both ends.

Solution studies (Dancker et al., 1975; Estes et al., 1981) and electron microscopy (Coluccio & Tilney, 1984) both suggested that phalloidin stabilizes actin filaments by inhibiting subunit dissociation at both ends of filaments. The EM assays also suggested that phalloidin might alter subunit association, at least at the barbed end. We have confirmed that phalloidin reduces the rate constants for subunit dissociation to near zero at both ends and also inhibits subunit association at the barbed

† This work was supported by Grant GM-26338 from the National Institutes of General Medical Sciences.

[1] Abbreviations: CB, cytochalasin B; CD, cytochalasin D.

0006-2960/91/0430-1973$02.50/0 © 1991 American Chemical Society

end by about 50%. These effects of phalloidin can be explained by a conformational change at the barbed end of polymerized actin molecules that strengthens their interaction with the adjacent subunit but that is unfavorable for the binding of a free monomer.

We also show how the effects of pH on the elongation rate constants account for the slower rate and higher critical concentration for actin polymerization at alkaline pH.

Materials and Methods

Cytochalasins B and -D were purchased from Sigma Chemical Co., St. Louis, MO. Phalloidin was purchased from Boehringer Mannheim, W. Germany. Fresh sperm were collected from *Limulus polyphemus* and acrosomal processes isolated by a modification (Pollard, 1986) of the method of Tilney (1975) and used the same day. The processes were pelleted and resuspended in 2× KM buffer (100 mM KCl, 20 mM imidazole, and 2 mM $MgCl_2$ at either pH 7.5, 6.6, or 8.3) with appropriate 2× concentrations of CB, CD, or phalloidin and were incubated for 10–15 min at 25 °C. Actin was prepared from rabbit muscle acetone powder according to Spudich and Watt (1971), purified by gel filtration on Sephacryl S-300 in buffer G (2 mM Tris, 0.2 mM ATP, 0.5 mM dithiothreiol, and 0.1 mM $CaCl_2$), and used within 1 week. Mg-ATP–actin was prepared by adding 50 μM $MgCl_2$ and 150 μM EGTA and incubating for 20 min at 2 °C. Mg-ADP–actin was prepared by the Selden et al. (1986) and Pollard (1986) modifications of the method of Pollard (1984) by incubating Mg-ATP–actin with 20 units/mL yeast hexokinase and 1 mM glucose for 4 h at 4 °C.

The elongation experiments were carried out in small droplets on parafilm exactly as described by Pollard (1986). Glow-discharged grids were placed on a 15-μL drop of acrosomal processes in 2× KM buffer containing the specified concentrations of CB, CD, or phalloidin, and the reaction was started by injecting into the drop an equal volume of actin monomers. The final assembly solutions contained 50 mM KCl, 10 mM imidazole, 1 mM Tris, 0.1 mM ATP or ADP, 1 mM $MgCl_2$, 0.05 mM $CaCl_2$, 1 mM EGTA, and 0.25 mM dithiothreiol, at pH 7.5, 6.6, or 8.3. Each reaction was terminated by draining the grid and inverting it onto a large drop of 50 mM spermine in 2× KM buffer to dilute the monomers and aggregate the filaments into bundles to facilitate measurement of their length. The grid was then stained for about 2 s with 1% uranyl acetate. The length of the newly polymerized actin was then measured on 15–20 acrosomal processes on the viewing screen of a JEOL 100CX electron microscope. The polarity of the acrosomal processes was established by their tapered morphology, the narrower end beng the barbed end (Tilney et al., 1981).

Results

Cytochalasin. Cytochalasins B and D inhibit the growth of ATP and ADP actin filaments at the barbed end more strongly than at the pointed end, but there is slow growth at the barbed end even at the highest cytochalasin concentrations tested (Figure 1; CB data not illustrated). This confirms the observation of Bonder and Mooseker (1986) made in 2 μM CB. The elongation rate at the barbed end is relatively independent of the concentration of cytochalasin between 1 and 10 μM. For ATP–actin, four experiments gave a mean slope of $-0.16\ s^{-1}\ \mu M^{-1}$ (SD = 0.08) corresponding to a 0.3% inhibition/μM CD. For ADP–actin, two experiments gave a mean slope of $-0.25\ s^{-1}\ \mu M^{-1}$ or 1.1% inhibition/μM CD between 1 and 10 μM. The semilog plot in Figure 1A tends to overemphasize these small changes. Note that although

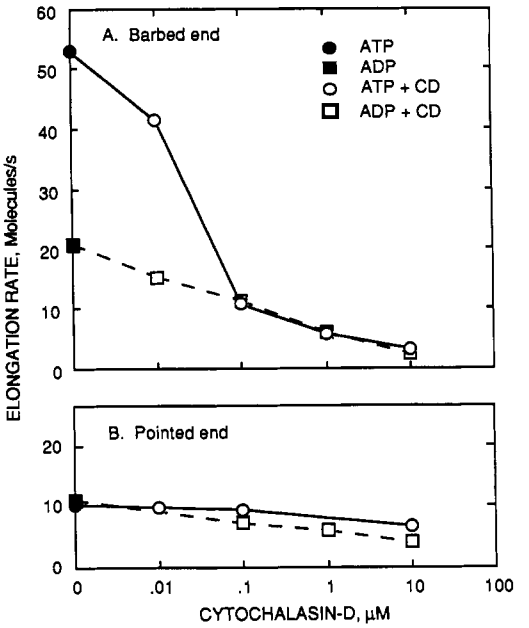

FIGURE 1: Dependence of the elongation rate on the concentration of cytochalasin D for either ATP–actin (●, ○) or ADP–actin (■, □). (A) Barbed end. (B) Pointed end. Conditions: 8 μM actin monomers, 50 mM KCl, 1 mM $MgCl_2$, 10 mM imidazole, 0.05 mM ATP or ADP, 1.1 mM EGTA, 1 mM Tris, 0.05 mM $CaCl_2$, pH 7.5 at 22 °C.

the elongation rate of ATP–actin is much faster than ADP–actin without CD, the rates are the same at high concentrations of CD (Figure 1A) and CB (not illustrated). The cytochalasin concentrations for half-maximal inhibition of the rate of elongation at the barbed end are 0.1 μM CB and 0.02 μM CD for ATP–actin and 0.1 μM CD for ADP–actin. CD also inhibits elongation at the pointed end by both ATP– and ADP–actin but to a lesser extent (Figure 1B).

At concentrations of 2 μM, both CB and CD alter the dependence of the rate of elongation at both ends of the filament on the concentrations of either ADP–actin (Figure 2A) or ATP–actin (Figure 2B and Table I). At the barbed end, the slope of plots of rate versus actin concentration is reduced by about 95% for ATP–actin and 82% for ADP–actin. The y intercept is reduced by 92% for ATP–actin and 98% for ADP–actin, so that the critical concentrations (x intercepts) are nearly the same as controls. At the pointed end, the slopes for both ATP– and ADP–actin are reduced about 50% by cytochalasin (Figure 2C). Slow growth of filaments at low actin monomer concentrations (<1–2 μM) made precise measurements of the critical concentrations difficult at the pointed end.

Phalloidin. The most striking effect of phalloidin on the elongation of actin filaments is a change in the y intercepts of plots of rate versus actin concentration at both ends of the filament (Figure 3, Table I). This confirms the observations of Dancker et al. (1975), Estes et al. (1981), and Coluccio and Tilney (1984). In KCl and $CaCl_2$ without $MgCl_2$, the critical concentrations and dissociation rate constants (y intercepts) are high enough to obtain accurate data on subtle changes. The measured values of the y intercepts were <10% of the control values, but they were reproducibly not zero as previously reported (Coluccio & Tilney, 1984). Consequently, the critical concentrations at both ends are very low but not zero. A second consistent effect of phalloidin is a reduction by 40–50% of the slope of plots of rate of elongation at the barbed end versus actin concentration as suggested by the data of Coluccio and Tilney (1984). At the pointed end the slope is not affected by phalloidin. In a single experiment in KCl and

Table I: Rate Constants for Actin Filament Elongation and Apparent Rate Constants in the Presence of Cytochalasins or Phalloidin[a]

conditions	barbed end			pointed end		
	k_+ (μM^{-1} s^{-1})	k_- (s^{-1})	A_1 (μM)	k_+ (μM^{-1} s^{-1})	k_- (s^{-1})	A_1 (μM)
KCl, $MgCl_2$, EGTA buffer						
ATP-actin (n = 5)	9.2	2.2	0.2	0.9	0.6	0.6
ATP-actin + 2 μM CB (n = 4)	1.0	0.7	0.7	0.4	0.2	0.5
ATP-actin + 2 μM CD (n = 3)	0.7	0.5	0.6	0.4	0.2	0.5
ADP-actin (n = 1)	3.9	6.1	0.7	1.0	0.9	0.9
ADP-actin + 2 μM CD (n = 1)	0.9	0.6	0.6	0.4	0.4	1.0
KCl, Ca buffer (n = 2)						
ATP-actin	6.2	7.3	1.2	0.8	1.1	1.7
ATP-actin + 10 μM phalloidin	3.2	0.9	0.3	0.9	0.1	0.1

[a] The constants were obtained from the slopes and intercepts of plots of elongation rate vs actin monomer concentration. A_1 refers to the critical concentration for polymerization, the x intercept of these plots. The values for experiments in the presence of cytochalasin or phalloidin are apparent rate constants, since the observed rates are the results of reactions in addition to the association and dissociation of subunits. The values given are means in the cases where multiple experiments (n) were completed.

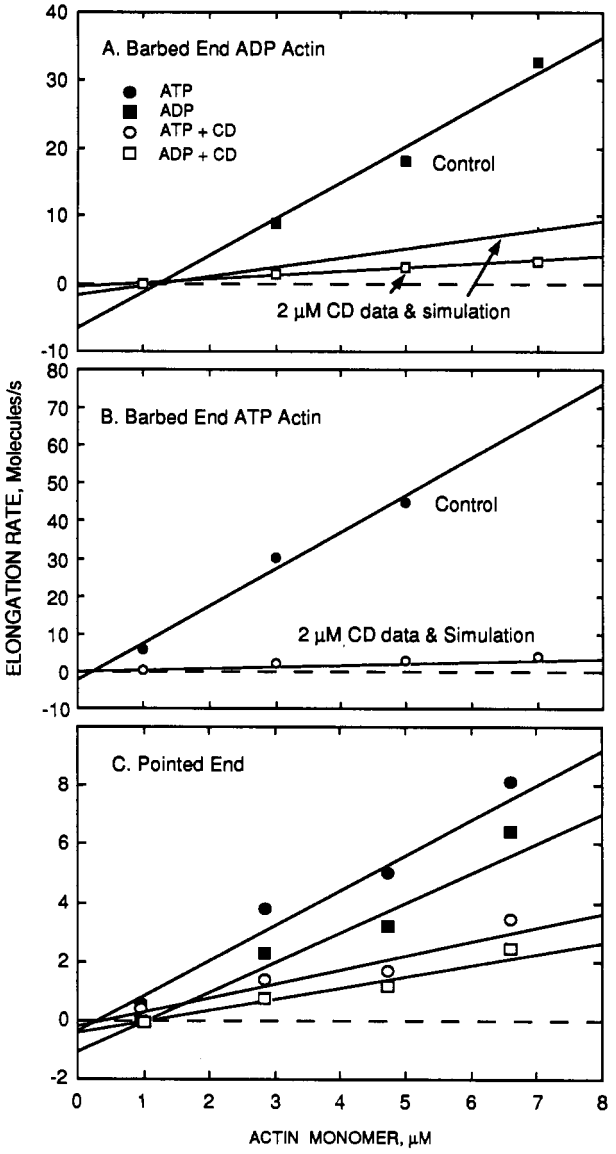

FIGURE 2: Dependence of the elongation rate on actin monomer concentration without (closed symbols) or with (open symbols) 2 μM cytochalasin D. (A) Barbed end with ADP-actin monomers. (B) Barbed end with ATP-actin monomers. (C) Pointed end with ATP-actin (●, ○) or ADP-actin (■, □). Conditions: 50 mM KCl, 1 mM $MgCl_2$, 10 mM imidazole, 0.05 mM ATP or ADP, 0.05 mM $CaCl_2$, 1.1 mM EGTA, 1 mM Tris, pH 7.5 at 25 °C. The lines are linear least-squares fits to the experimental data except the lines marked simulation in (A) and (B). The simulation lines were calculated by kinetic modeling using model 2 for ADP-actin and model 5 for ATP-actin with the rate and equilibrium constants given in Table II.

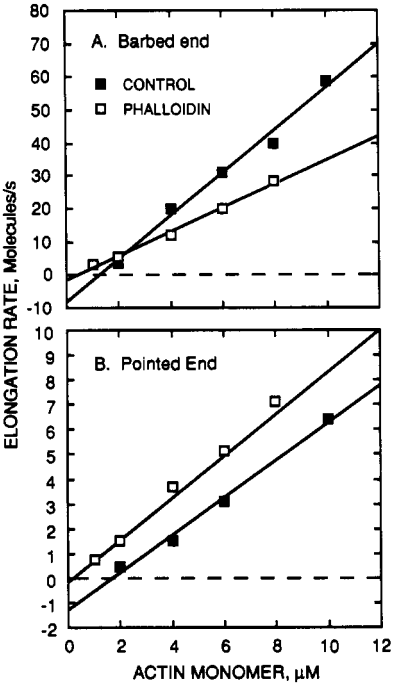

FIGURE 3: Effect of phalloidin on the dependence of the elongation rate on the concentration of ATP-actin monomers. (A) Barbed end. (B) Pointed end. Conditions: 50 mM KCl, 10 mM imidazole, 1 mM Tris, 1 mM $CaCl_2$, 0.1 mM ATP, 0.25 mM dithiothreitol, pH 7.5 at 25 °C. Control (■); 10 μM phalloidin (□).

$MgCl_2$, 10 μM phalloidin reduced the slope by 75% at the barbed end and by less than 20% at the pointed end.

pH. Studies on actin polymerization have been carred out at different pHs in various laboratories, but remarkably there is no direct information available on how pH affects the elongation rate constants. Consequently, we examined elongation over the range of pHs from 6.6 to 8.3. At the extremes of the range tested, pH has no effect on the association rate constant for elongation at the barbed end, but the dissociation rate constant is larger at alkaline pH (Figure 4A). Accordingly, the critical concentration is higher at alkaline pH. At the pointed end (Figure 4B), the critical concentrations are nearly the same at pH 6.6 and 8.3, but the association rate constant is 35% lower at pH 8.3 than pH 6.6.

Discussion

Cytochalasins Inhibit but Do Not Stop Elongation at Both Ends of the Actin Filament. In this paper, we have confirmed that CD and CB each inhibit monomer addition at both ends of actin filaments but that even 10 μM CD does not stop growth at either end completely. By comparing the effects

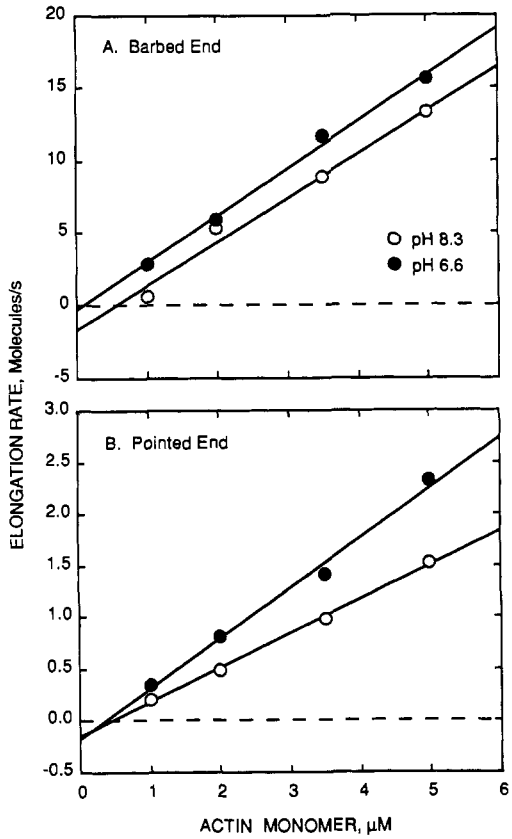

FIGURE 4: Effect of pH on the dependence of the elongation rate on the concentration of ATP-actin monomer. (A) Barbed end. (B) Pointed end. Conditions: 50 mM KCl, 1 mM $MgCl_2$, 10 mM imidazole, 0.05 mM ATP, 1 mM Tris, and 0.05 mM $CaCl_2$ at 25 °C. (●) pH 6.6; (O) pH 8.3.

of the cytochalasins on ATP-actin and ADP-actin, we show that ATP-actin assembles much like ADP-actin at micromolar concentrations of cytochalasin. These results disprove the simple barbed end capping mechanism but can be explained reasonably well by a hybrid mechanism that includes the effects of low-affinity binding of cytochalasins to ATP-actin monomers (Godette & Frieden, 1986a,b).

Computer Modeling of the Mechanism of Action of Cytochalasins at the Barbed End of Filaments. We used the kinetics simulation program KINSIM (Barshop et al., 1983) to test various mechanisms for their ability to fit our elongation rate data as a function of the concentrations of both actin and cytochalasin. The conclusions are easiest to understand if we start with the dependence of the elongation rate of ADP-actin at the barbed end on the concentration of CD (Figures 1A and 5A) and then apply those conclusions to the more complicated situation of the elongation of ATP-actin in the presence of CD. All of the calculations have been made for CD but should apply equally well for CB with some adjustment of the values of the rate and equilibrium constants.

(1) Simple Capping. The widely accepted simple capping model cannot explain the dependence of the rate of elongation on the concentration of CD (Figure 5A). In such a model, there are only two reactions:

$$AD + Bend == Bend+1 \quad (1)$$

$$CD + Bend = BendCD \quad (2)$$

where AD is actin-ADP, Bend is the barbed end, and CD is cytochalasin D. In these and subsequent equations, a single "equals" symbol (=) represents a rapid equilibrium, and double "equals" (==) represent association and dissociation reactions for which rate constants are specified. Reaction 1 is simply

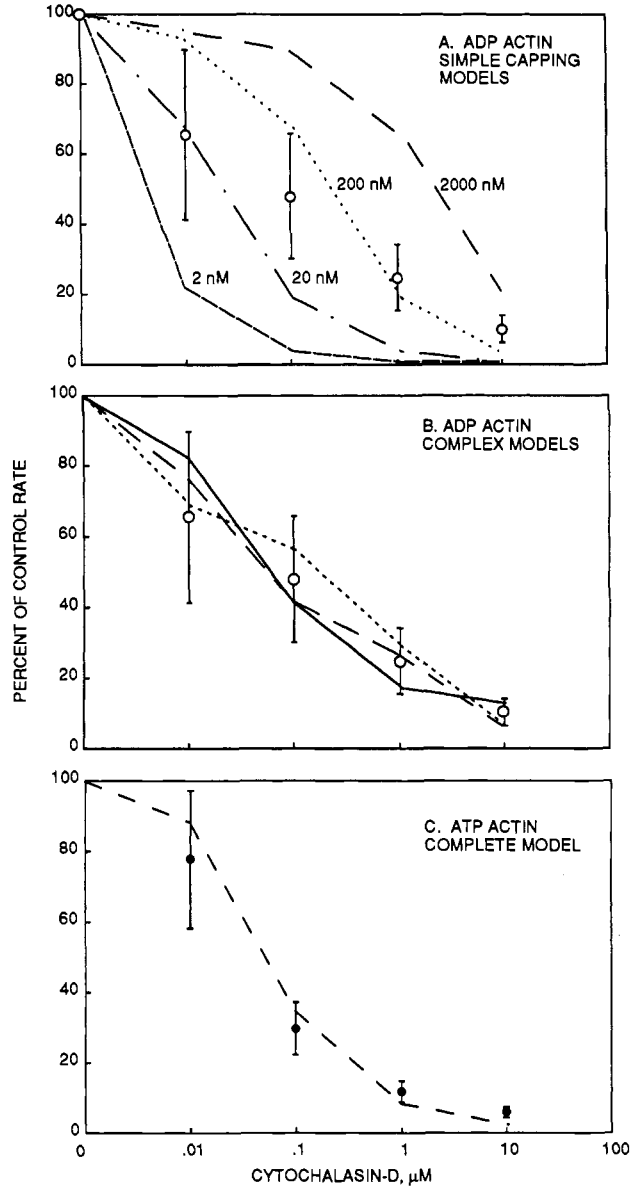

FIGURE 5: Theoretical curves for the dependence of the elongation rate at the barbed end of actin filaments upon the concentration of cytochalasin D. The experimental data ± 1 standard deviation of the length distribution are reproduced from Figure 1. (A) Attempts to fit the data for ADP-actin with the simple capping mechanism (model 1 in the text) with a range of equilibrium constants K2 for CD binding to the barbed end. The four theoretical curve from left to right correspond to K2 = 2, 20, 200, and 2000 nM. (B) Theoretical curves for elongation by ADP-actin calculated by using three different mechanisms: the solid line is the incomplete capping (model 2 in the text); the dotted line is capping by two CD's (model 3 in the text); and the dashed line is incomplete capping with monomer inactivation (model 4 in the text). The details of these mechanisms are discussed in the text. The rate and equilibrium constants are given in Table II and in the text. (C) Comparison of experimental data for elongation by ATP-actin with a theoretical curve calculated by kinetic stimulation using model 5, a mechanism that includes rapid hydrolysis of ATP by CD-actin dimers and partial capping of barbed ends. The rate and equilibrium constants are given in Table II.

the association and dissociation of AD at the barbed end. Reaction 2 is the binding of CD to the barded end and is considered here as a rapid equilibrium. In a simple capping mechanism, it is assumed that the BendCD complex cannot bind or dissociate an AD subunit. Given this mechanism and the rate constants from Figure 2A, we calculated theoretical curves for the time course of elongation at the barbed end in the presence of 8 μM ADP-actin over a range of equilibrium

Table II: Rate and Equilibrium Constants for the Assembly of ATP–Actin in the Presence of 2 μM Cytochalasin D[a]

constant	value	reference
k_{+1} (μM^{-1} s^{-1})	4	measured in Figure 2
k_{-1} (s^{-1})	6	measured in Figure 2
$K2$ (μM)	0.002	Flanagan & Lin (1980)
k_{+3} (μM^{-1} s^{-1})	1	modeled in Figure 5B
k_{-3} (s^{-1})	0.1	modeled in Figure 5B
$K4$ (μM)	2.5	Godette & Frieden (1986b)
$K5$ (μM)	0.5	Godette & Frieden (1986b)
k_{+6} (s^{-1})	5	Godette & Frieden (1986b)
k_{-6} (s^{-1})	0.75	Godette & Frieden (1986b)
$K7$ (μM)	0.5	modeled in Figure 5C
k_{+8} (s^{-1})	0.01	Frieden & Patane (1988)
k_{-8} (s^{-1})	0	assumed
k_{+9} (μM^{-1} s^{-1})	10	Pollard (1986)
k_{-9} (s^{-1})	1	Pollard (1986)
$K10$ (μM)	1	Godette & Frieden (1985)

[a] Model 5, rapid hydrolysis by CD–actin dimers, and partial capping of barbed ends.

constants for the second reaction. No K_d in the range of 2–2000 nM gives elongation rates that fit the observed dependence on the concentration of CD (Figure 5A).

Any model with CD binding to a single site that totally inhibits subunit association and dissociation suffers from two problems. First, titration of a single site will give a sigmoidal curve on a semilog plot in contrast to the more linear relationship that we observed. Second (and more definitively), complete capping is inconsistent with the residual growth that we and Bonder and Mooseker (1986) observed even at high concentrations of cytochalasin. These problems suggest that there must be at least two different reactions involving CD and that they must have substantially different equilibrium constants. We investigated three different possibilities, all of which gave good fits to the observations. All of these models involve binding of CD to a site on the barbed end of the filament plus one additional site. Although these models cannot be distinguished by currently available data, they are useful because they make specific predictions about reactions of CD with actin that can be explored in the future.

(*2*) *Incomplete Capping.* The more complex model suggests that binding of CD to a barbed end only *partially caps* the end with respect to the association and dissociation of AD subunits:

$$\text{AD} + \text{Bend} = = \text{Bend+1} \quad (1)$$

$$\text{CD} + \text{Bend} = \text{BendCD} \quad (2)$$

$$\text{AD} + \text{BendCD} = = \text{BendCD+1} \quad (3)$$

Providing that the rate constants for step 3 are substantially less (such as 10-fold) than those for step 1, the equilibrium constant for step 2 can be adjusted (Table II) to give an acceptable fit of the model to the experimental data (Figure 5B). These same constants yield theoretical curves that closely fit to the dependence of the elongation rate in 2 μM CD on the ADP–actin concentration (Figure 2A). The best fits were obtained with kinetic constants where ADP–actin binds to and dissociates from capped ends of actin filaments one-tenth as fast as these reactions with free ends.

This partial capping is particularly attractive since it is well documented (Flanagan & Lin, 1980) that CD binds to actin filaments with a nanomolar dissociation constant, so that the polymers elongating in micromolar concentrations of CD *must* have CD bound to their barbed ends. By definition, such filaments are not completely capped. This model is incomplete in the sense that the properties of BendCD+1 are not specified. Is such a filament no longer capped? What becomes of the CD now bound to the penultimate subunit? The answers to these questions make little difference to the modeling of initial rates, since reaction 2 is considered to be a rapid equilibrium that would immediately recap the end of the filament, but would be a factor in modeling a complete time course of assembly. However, it seems likely that CD has a low affinity for (and therefore dissociates rapidly from) internal actin subunits, since no one has ever detected binding of cytochalasins to more than a few sites on actin filaments.

(*3*) *Capping by Two Cytochalasins.* Another complex mechanism postulates binding of CD to two distinct sites (such as each of the two terminal subunits) at the barbed end of the filament with *partial capping when only one site is occupied*:

$$\text{AD} + \text{Bend} = = \text{Bend+1} \quad (1)$$

$$\text{CD} + \text{Bend} = \text{BendCD} \quad (2)$$

$$\text{AD} + \text{BendCD} = = \text{BendCD+1} \quad (3)$$

$$\text{CD} + \text{BendCD} = \text{Bend2CD} \quad (4)$$

It is assumed that AD binds to BendCD but not to Bend2CD. By adjusting the equilibrium constants such that $K_d(2)$ = 2 nM and $K_d(3)$ = 1000 nM and assuming that the association rate constant for eq 4 is one-third of that for eq 1, the model gives a reasonable fit to the experimental data (Figure 5B). Binding of two CD's to the barbed end of filaments has never been seriously considered, but is consistent with the available binding data, since within a factor of 2 the number of filaments has never been accurately known in these experiments (Flanagan & Lin, 1980). As in the second model, the fate of the cytochalasins bound to internal subunits (produced by reaction 3) is not specified, but they are expected to dissociate rapidly. Reasonable kinetic constants with CD binding with low affinity to the second site [$K_d(4)$ = 1 μM] allow this model to fit the experimental data nearly as well as model 2 (Figure 5B). One possibility is that there is a gradient of affinity for cytochalasin at the barbed end of the filament with a high-affinity site on the terminal subunit, a moderate-affinity site on the penultimate subunit, and weak sites on all other subunits.

(*4*) *Incomplete Capping plus Monomer Inactivation.* An even more complex model involves *partial capping* when CD binds to the barbed end coupled with *inactivation of AD monomers by binding CD.* This is an example of how additional steps can be added to a model (in this case model 2) in an effort to improve the fit to the experimental data:

$$\text{AD} + \text{Bend} = = \text{Bend+1} \quad (1)$$

$$\text{CD} + \text{Bend} = \text{BendCD} \quad (2)$$

$$\text{AD} + \text{BendCD} = = \text{BendCD+1} \quad (3)$$

$$\text{AD} + \text{CD} = \text{ADCD} \quad (4)$$

The first thre steps are identical with model 2. The fourth step is the binding of CD to ADP–actin in a rapid equilibrium as shown by Godette and Frieden (1986a). It is assumed that the complex ADCD cannot bind to the end of actin filaments. As expected for any model with additional variables, the rate and equilibrium constants can be adjusted to give a slightly better fit to the experimental data than the model without step 4 (Figure 5B).

(*5*) *A Complex Model Explains Elongation by ATP–Actin in the Presence of Cytochalasin D.* By combining the partial capping model for ADP–actin with the moderate affinity binding of CD to ADP–actin and the effects of cytochalasins on the dimerization and nucleotide hydrolysis of ATP–actin (Godette & Frieden, 1986a,b), we found a model and kinetic

constants that are consistent with the dependence of the elongation of ATP-actin filaments on both the concentrations of CD (Figure 5C) and ATP-actin monomers (Figure 2B). In the example illustrated, we used the partial capping model. We did not formally test the second model using capping by two cytochalasins but expect that similar results would be obtained. The model requires 10 different reactions:

$$\text{AD + Bend = = Bend+1} \quad (1)$$

$$\text{CD + Bend = BendCD} \quad (2)$$

$$\text{AD + BendCD = = BendCD+1} \quad (3)$$

$$\text{AT + CD = ATCD} \quad (4)$$

$$\text{AT + ATCD = ATATCD} \quad (5)$$

$$\text{ATATCD = = ADATCD} \quad (6)$$

$$\text{ADATCD = ATCD + AD} \quad (7)$$

$$\text{AD = = AT} \quad (8)$$

$$\text{AT + Bend = = Bend+1} \quad (9)$$

$$\text{AD + CD = ADCD} \quad (10)$$

Reactions 1–3 and 10 are simply the incomplete capping model from above. Reactions 4–7 were originally described by Godette and Frieden (1986a,b) to account for the effects of CD on ATP-actin monomers. Reaction 8 is the exchange of nucleotide on monomeric actin (simplified to one step), and reaction 9 is the elongation by ATP-actin monomers. We assume that ATP-actin does not bind to barbed ends capped by CD.

Such a large number of reactions may appear unnecessarily complicated, but most of them have been observed and evaluated independently (Tables I and II). Consequently, the kinetic modeling was constratined by literature values for reactions 1, 2, 4–9, and 10. We assumed $k_8 = 0.01\ s^{-1}$ based on Frieden and Patane (1988) and $k_{-8} = 0$ since the concentration of ADP in the reaction was very low. For reactions 3 and 10, we used the values obtained from the modeling for ADP-actin in the previous section. This left the equilibrium constant for reaction 7 as the only variable.

We found that a value of 0.5 μM for $K_d(7)$ along with the other values gave a good fit to the dependence of the reaction on the concentrations of both CD (Figure 5C) and ATP-actin (Figure 2B). This agreement includes features that have previously been difficult to explain such as the continued slow growth of filaments in apparently saturating concentrations of cytochalasins (Figure 1A) and the minimal effect of cytochalasin on the critical concentration for elongation of ATP-actin (Figure 2B). Thus, the full range of postulated reactions of actin monomers and filaments with CD not only is necessary but also is sufficient to account for the effects of CD on elongation.

A KINSIM simulation of a typical time course is helpful in understanding the mechanism (Figure 6A). KINSIM not only calculates the time course of incorporation of subunits at the end of the actin filament but also calculates the concentrations of all intermediates. Within seconds after 8 μM ATP-actin is mixed with 1 μM CD, most of the actin is converted to ADP-actin. CD acts catalytically through reactions 4–7 to form AT dimers that hydrolyze ATP bound to one of the dimer subunits and then dissociate as originally discovered by Godette and Frieden (1986a,b). Consequently, after about 5 s, ADP-actin is the major species available to add to the barbed end of filaments. As a consequence, the rate of elongation is less than that for ATP-actin, but more importantly, the reaction goes on even at ends capped with CD, owing to the partial capping with respect to ADP-actin subunits described above (Figure 5B). These features account for the low rate of elongation by ATP-actin even under conditions where most of the barbed ends are capped with CD. A nonintuitive feature of this mechanism is illustrated in Figure 6B. The maximum concentration of ADP-actin does not occur at the highest catalyst (CD) concentration. Instead, the maximum occurs at about 1 μM CD. Higher concentrations of CD shift reaction 4 to the right and the equilibrium of step 7 to the left. Consequently, dimers become a major species at high concentrations of CD.

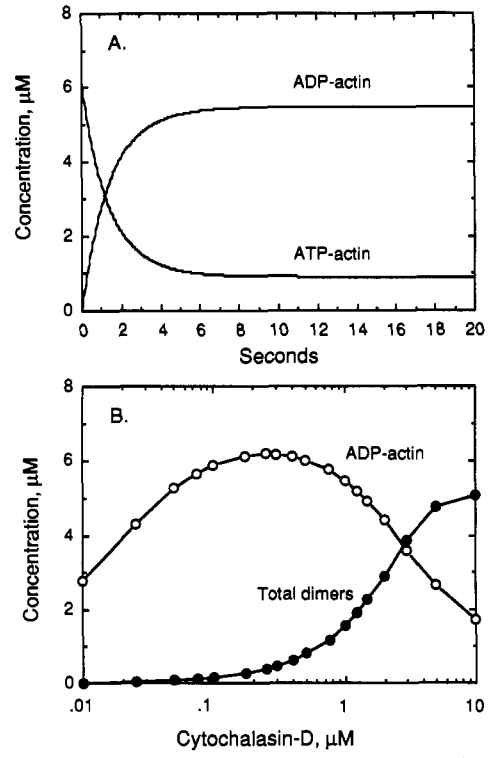

FIGURE 6: Kinetic simulation of the reaction of ATP-actin with CD using reactions 4–8 from model 5 and the constants from Table II. (A) Theoretical kinetic curves for the concentrations of ATP-actin and ADP-actin after mixing 8 μM ATP-actin with 1 μM CD. (B) Dependence of the maximum concentration of ADP-actin (○) and total actin dimer species (●) upon the concentration of CD.

In this model, it is assumed that barbed ends capped with CD do not bind or dissociate ATP-actin subunits; that is, they are completely capped. An alternative model could include association and dissociation of ATP-actin with rate constants substantially less than those for uncapped ends. We did not test this model because the reaction would only make a small contribution to elongation under conditions where most of the ATP-actin monomers are converted to ADP-actin. Nonetheless, we think that inclusion of this step is reasonable and that it might improve the agreement between the model and the data.

Mechanism of Action of Cytochalasin at the Pointed End of Actin Filaments. We have not yet been able to identify a mechanism to explain the inhibition of polymerization at the pointed end of actin filaments. In agreement with Bonder and Mooseker (1986), we find that CD also inhibits the elongation at the pointed end of actin filaments (Figures 1B and 2C). Both ATP-actin and ADP-actin are inhibited about 50% at high concentrations of CD. We tested by computer simulation of kinetics some simple models where CD binds to ADP-actin monomers and prevents or partially inhibits their incorporation at the pointed end of filaments. Since we did not obtain good

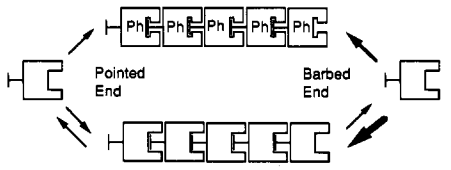

FIGURE 7: Diagrammatic model for the effects of phalloidin (Ph) on the elongation of actin filaments. The arrows reflect the size of the rate constants. When phalloidin binds to subunits in the polymer, the rate of subunit dissociation from both ends is reduced nearly to zero by a hypothetical conformational change at the barbed end of each subunit that gives them a higher affinity for the pointed end of the neighboring subunit. This change is shown to inhibit the rate of binding of phalloidin-free molecules at the barbed but not the pointed end of the filament.

fits of the experimental data even for ADP–actin, we did not attempt the more complex task of explaining the effects on ATP–actin. Since it is much more difficult to obtain accurate data on elongation at the pointed end than the barbed end, some limitations of the data may contribute to the apparent difficulty in its interpretation. We do suggest that whatever the mechanism for ADP–actin that it also accounts for the effects on ATP–actin which will be largely converted to ADP–actin in the presence of micromolar CD.

Implications of the Mechanism of Action of Cytochalasin for the Interpretation of Experiments on Live Cells. It is no longer necessary to attribute all of the effects of cytochalasins on cells to barbed end capping. The concentrations of cytochalasins typically used in cellular experiments also have strong effects on actin monomers and may convert much of a cell's monomeric actin to ADP–actin. On the other hand, even at saturating concentrations, cytochalasins do not completely block the barbed ends with respect to either subunit association or dissociation.

Even a complete account of the mechanism of action of cytochalasins on purified actin will provide only part of the information required to interpert the effects of cytochalasins on live cells. We still need to know how ADP–actin produced by cytochalasin and complexes of actin with cytochalasins interact with the full range of actin binding proteins present in cells. However, beyond evidence that *Acanthamoeba* profilins bind more strongly to ADP–actin than ATP–actin (Lal et al. 1985), little is known. Consequently, dramatic effects of cytochalasins such as those observed recently with advanced optical methods (Forscher & Smith, 1988) may arise from a currently unresolvable combination of effects of cytochalasin on the ends of actin filaments, the nucleotide composition of unpolymerized actin and the interaction of both polymerized and unpolymerized actin with their regulatory proteins.

Phalloidin Stabilizes Actin Filaments by Reducing the Rate of Dissociation of Subunits and Inhibiting Monomer Association at the Barbed End. We have confirmed the widely held belief that phalloidin stabilizes actin filaments by inhibiting subunit dissociation at both ends and focus here on the possible mechanism whereby phalloidin also inhibits subunit addition at the barbed end. Our data confirm the observation of Coluccio and Tilney (1984) that phalloidin reduces the association rate constant at the barbed end by about 50%. This might be explained by the same mechanism that inhibits subunit dissociation at both ends (Figure 7). The stabilization of filaments by phalloidin is likely to involve a conformational change at one (or more) interface between subunits in the polymer. This change presumably strengthens the bonds between the subunits and might be viewed as locking them together in some way. For argument, the barbed end of each subunit may lock onto the pointed end of the neighboring subunit. The most obvious consequence of such a lock is the stabilization of the polymer againt all sorts of insults, but an additional consequence may be that the barbed end of a filament saturated with phalloidin may be unfavorable for docking with an incoming subunit. This idea might be tested by the determination of the structure of the actin molecule with bound phalloidin.

The Dissociation Rate Constant Increases at Alkaline pH. The effects of pH on the elongation rate constants reported here and on the nucleation of actin filaments (Zimmerle & Frieden, 1988) are similar and may have the same underlying mechanisms. At pH 6.0, nucleation is favored because dimers are more stable by 3 orders of magnitude than at alkaline pH 8.0. In that case, the reaction was treated as a rapid equilibrium so it could only be conjectured that the increased stability of dimers at acid pH is due to a lower dissociation constant. For comparison, the elongation is faster at pH 6.6 than at pH 8.3 because at acid pH the dissociation rate constant at the barbed end is lower by a factor of about 10 and the association rate constant at the pointed end in larger by 35%. This suggests that both more favorable association and reduced dissociation of dimers at acid pH may contribute to the remarkable differences in their stability as a function of pH.

ACKNOWLEDGMENTS

We thank D. Wachsstock and I. Goldberg for help with Figure 6.

REFERENCES

Barshop, B. A., Wrenn, R. F., & Frieden, C. (1983) *Anal. Biochem. 130*, 134–145.
Bonder, E. M., & Mooseker, M. S. (1986) *J. Cell Biol. 102*, 282–288.
Brenner, S. L., & Korn, E. D. (1979) *J. Biol. Chem. 254*, 9982–9985.
Brown, S. S., & Spudich, J. A. (1979) *J. Cell Biol. 83*, 657–662.
Carlier, M.-F., Criquet, P., Pantaloni, D., & Korn, E. D. (1986) *J. Biol. Chem. 261*, 2041–2050.
Coluccio, L. M., & Tilney, L. G. (1984) *J. Cell Biol. 99*, 529–535.
Cooper, J. A. (1987) *J. Cell Biol. 105*, 1473–1478.
Dancker, P., Low, I., Hasselbach, W., & Wieland, Th. (1975) *Biochim. Biophys. Acta 400*, 407–414.
Estes, J. E., Selden, L. A., & Gershman, L. C. (1981) *Biochemistry 20*, 708–712.
Flanagan, M. D., & Lin, S. (1980) *J. Biol. Chem. 255*, 835–838.
Forscher, P., & Smith, S. J. (1988) *J. Cell Biol. 107*, 1505–1516.
Frieden, C., & Patane, K. (1988) *Biochemistry 27*, 3812–3820.
Goddette, D. W., & Frieden, C. (1985) *Biochem. Biophys. Res. Commun. 128*, 1087–1092.
Goddette, D. W., & Frieden, C. (1986a) *J. Biol. Chem. 261*, 15970–15973.
Goddette, D. W., & Frieden, C. (1986b) *J. Biol. Chem. 261*, 15974–15980.
Lal, A. A., & Korn, E. D. (1985) *J. Biol. Chem. 260*, 10132–10138.
Lin, D. C., Tobin, K. D., Grumet, M., & Lin, S. (1980) *J. Cell Biol. 84*, 455–460.
MacLean-Fletcher, S., & Pollard, T. D. (1980) *Cell 20*, 329–341.
Pollard, T. D. (1984) *J. Cell Biol. 99*, 769–777.

Pollard, T. D. (1986) *J. Cell Biol. 103*, 2747–2754.
Pollard, T. D., & Mooseker, M. S. (1981) *J. Cell Biol. 88*, 654–659.
Selden, L. A., Gershman, L. C., & Estes, J. E. (1986) *Biophys. J. 49*, 454a.
Spudich, J. A., & Watt, S. (1971) *J. Biol. Chem. 246*, 4866–4871.
Tilney, L. G. (1975) *J. Cell Biol. 64*, 289–310.
Tilney, L. G., Bonder, E. M., & DeRosier, D. J. (1981) *J. Cell Biol. 90*, 485–494.
Zimmerle, C. T., & Frieden, C. (1988) *Biochemistry 27*, 7766–7772.

Activity and Structure of the Active-Site Mutants R386Y and R386F of *Escherichia coli* Aspartate Aminotransferase†

Avis T. Danishefsky,‡ James J. Onnufer,§ Gregory A. Petsko,‖ and Dagmar Ringe*,‖
Department of Chemistry, Massachusetts Institute of Technology, Cambridge, Massachusetts 02139
Received August 3, 1990; Revised Manuscript Received November 13, 1990

ABSTRACT: Arginine-386, the active-site residue of *Escherichia coli* aspartate aminotransferase (EC 2.6.1.1) that binds the substrate α-carboxylate, was replaced with tyrosine and phenylalanine by site-directed mutagenesis. This experiment was undertaken to elucidate the roles of particular enzyme–substrate interactions in triggering the substrate-induced conformational change in the enzyme. The activity and crystal structure of the resulting mutants were examined. The apparent second-order rate constants of both of these mutants are reduced by more than 5 orders of magnitude as compared to that of wild-type enzyme, though R386Y is slightly more active than R386F. The 2.5-Å resolution structure of R386F in its native state was determined by using difference Fourier methods. The overall structure is very similar to that of the wild-type enzyme in the open conformation. The position of the Phe-386 side chain, however, appears to shift with respect to that of Arg-386 in the wild-type enzyme and to form new contacts with neighboring residues.

Aspartate aminotransferase plays a central role in amino acid metabolism by catalyzing the interconversion L-aspartate + α-ketoglutarate ⇄ L-glutamate + oxaloacetate. This enzyme is the most extensively studied of the aminotransferases and has been well characterized in terms of both physical and enzymatic properties. The reaction is catalyzed via a ping-pong Bi-Bi mechanism in which the essential cofactor converts between the pyridoxal phosphate and pyridoxamine phosphate form (Velick & Vavra, 1962). X-ray crystallographic studies have been carried out on L-aspartate aminotransferase (L-AspAT)[1] derived from various sources including chicken mitochondrion (Ford et al., 1980; Kirsch et al., 1984; Jansonius et al., 1985), chicken cytoplasm (Borisov et al., 1980), pig cytoplasm (Arnone et al., 1985), and *Escherichia coli* (Kamitori et al., 1988; Smith et al., 1989). The overall polypeptide fold has been found to be similar for all of these species, and all active-site residues are conserved (Kondo et al., 1987). The active enzyme is an α_2 dimer. As shown in Figure 1, each subunit consists of two domains. The large domain, which binds the PLP cofactor, encompasses residues 48–325. The small domain is defined as residues 15–47 and 326–410. Two independent active sites of the dimer are located at the cleft between the two domains, and each is comprised of residues from both subunits. High-resolution X-ray crystallographic studies (Kirsch et al., 1984; Arnone et al., 1985; Borisov et al., 1985; Harutyunyan et al., 1985; Smith et al., 1989) in conjunction with site-directed mutagenesis studies (Malcolm & Kirsch, 1985; Cronin & Kirsch, 1988; Toney & Kirsch, 1987; Hayashi et al., 1989; Inoue et al., 1989; Hayashi et al., 1990) have helped to elucidate the roles of several of the active-site residues. Specificity for dicarboxylic acids appears to be imparted by two active-site arginines. Arginine-386 in the small domain interacts with the α-carboxylate of the substrate. Arginine-292[2], (see footnote 2) located in the large domain of the other subunit, interacts with the side-chain carboxylate.

It has been observed in solution studies (Gehring & Christen, 1978; Pfister et al., 1978) as well as by X-ray crystallographic analyses (Kirsch et al., 1984; S. C. Almo and A. T. Danishefsky, unpublished results) that the enzyme undergoes a conformational change upon binding dicarboxylic acid substrates or inhibitors. This motion can be modeled, based on crystal structures of the open and closed forms, as a rigid-body rotation of the small domain with respect to the large domain, resulting in the closing of the enzyme around the substrate. Similar substrate-induced conformational changes have been observed in other enzyme systems, including

† This work was supported by grants from the NIH (GM26788 to D.R. and G.A.P. and GM 11821 to A.T.D.).
* Author to whom correspondence should be addressed at Brandeis University, Rosensteil Basic Medical Sciences Research Center, Waltham, MD 02254-9110.
‡ Present address: National Cancer Institute, Frederick Cancer Research Facility, P.O. Box B, Frederick, MD 21702.
§ Present address: Department of Biochemistry, University of California, Berkeley, CA 94720.
‖ Present address: Brandeis University, Rosensteil Basic Medical Sciences Research Center, Waltham, MA 02254-9110.

[1] Abbreviations: L-AspAT, L-aspartate aminotransferase; PLP, pyridoxal 5′-phosphate; TAPS, *N*-[tris(hydroxymethyl)methyl]-3-aminopropanesulfonic acid; rms, root-mean-square; $R_{sym} = \sum_n\sum_i|I_i - \bar{I}|/\sum_n\sum_i|\bar{I}|$, where I_i is the ith observation of the nth reflection and $\bar{I}$ is the mean of all observations of the nth reflection.

[2] The superscript 2 denotes residues located on the second subunit of the dimer.

0006-2960/91/0430-1980$02.50/0 © 1991 American Chemical Society